Pharm Res (2014) 31:3136–3149
DOI 10.1007/s11095-014-1406-3

RESEARCH PAPER

New Thermoresistant Polymorph from CO_2 Recrystallization of Minocycline Hydrochloride

Miguel A. Rodrigues • João M. Tiago • Luis Padrela • Henrique A. Matos • Teresa G. Nunes • Lídia Pinheiro • António J. Almeida • Edmundo Gomes de Azevedo

Received: 7 January 2014 / Accepted: 28 April 2014 / Published online: 20 May 2014

ABSTRACT

Purpose To prepare and thoroughly characterize a new polymorph of the broad-spectrum antibiotic minocycline from its hydrochloride dehydrate salts.

Methods The new minocycline hydrochloride polymorph was prepared by means of the antisolvent effect caused by carbon dioxide. Minocycline recrystallized as a red crystalline hydrochloride salt, starting from solutions or suspensions containing CO_2 and ethanol under defined conditions of temperature, pressure and composition.

Results This novel polymorph (β-minocycline) revealed characteristic PXRD and FTIR patterns and a high melting point (of 247°C) compared to the initial minocycline hydrochloride hydrates (α-minocycline). Upon dissolution the new polymorph showed full anti-microbial activity. Solid-state NMR and DSC studies evidenced the higher chemical stability and crystalline homogeneity of β-minocycline compared to the commercial chlorohydrate powders. Molecular structures of both minocyclines present relevant differences as shown by multinuclear solid-state NMR.

Conclusions This work describes a new crystalline structure of minocycline and evidences the ability of ethanol-CO_2 system in removing water molecules from the crystalline structure of this API, at modest pressure, temperature and relatively short time (2 h), while controlling the crystal habit. This process has therefore the potential to become a consistent alternative towards the control of the solid form of APIs.

M. A. Rodrigues · J. M. Tiago · L. Padrela · H. A. Matos · T. G. Nunes · E. G. de Azevedo (✉)
Centro de Química Estrutural and Department of Chemical Engineering Instituto Superior Técnico, Universidade de Lisboa, Lisboa, Portugal
e-mail: egazevedo@tecnico.ulisboa.pt

L. Pinheiro · A. J. Almeida
Instituto de Investigação do Medicamento (i. Med.ULisboa) Faculdade de Farmácia, Universidade de Lisboa, Lisboa, Portugal

KEY WORDS Antisolvent effect · Minocycline · Physical stability · Structural characterization · Supercritical CO_2

ABBREVIATIONS

API	Active pharmaceutical ingredient
ASAIS	Atomization of supercritical antisolvent induced suspensions
DSC	Differential scanning calorimetry
FTIR	Fourier transform infrared spectroscopy
MRSA	Methicillin-resistant Staphylococcus aureus
Nl	Normal liter (mass of 1 l of gas at 1 atm and 20°C)
PR-EOS	Peng-Robinson equation of state
PXRD	Powder X-ray diffraction
RH	Relative humidity
RVC	Recrystallization visual cell
SAS	Supercritical antisolvent
SELTICS	Sideband elimination by temporary interruption of the chemical shift
αMH	Form α of minocycline hydrochloride
βMH	Form β of minocycline hydrochloride

INTRODUCTION

Minocycline is a broad-spectrum long-acting, semi-synthetic derivative of the antibiotic tetracycline, which inhibits the bacterial protein synthesis preventing the binding of aminoacyl-tRNA to the 30S bacterial ribosomal subunit. Among the several antibiotics for clinical use, minocycline (oral or intravenous administration) presents a broader spectrum when compared with other compounds from the tetracycline family. This antibiotic shows a relevant potential against bacterial multiresistant strains, such as methicillin-resistant S*taphylococcus aureus* (MRSA) and *Acinetobacter baumanii*, accountable for a high number of community- and hospital-acquired infections. In addition, it is most commonly used to

treat certain types of skin infections, mild rheumatoid arthritis, urinary tract infections, gallbladder infections, and respiratory tract infections, such as bronchitis, pneumonia, and sinusitis. Minocycline is the most liposoluble of its class, effectively crossing the blood–brain barrier. Recently neuroprotective properties in different neurodegenerative diseases have been related to minocycline's anti-inflammatory and anti-apoptotic effects. The increased lipophilicity also enhances minocycline penetration into various tissues when compared to other tetracyclines (1–3).

Minocycline is commercialized in the form of a hydrochloride dihydrate salt (4). However, hydrates may pose several drawbacks regarding products stability, particularly whenever the product has poor crystallinity. In most cases, higher water content is associated with higher rate of chemical degradation. The magnitude of the "water effect" depends mostly on the system being examined, as reviewed elsewhere (5,6). For example, formulation instability may result from the redistribution of water from a crystallizing API to the remaining amorphous component (s), or vice versa. Overall, the control of the crystalline form is crucial for pharmaceutical development and formulation. Polymorphic behavior should be acknowledged at an early stage of development as a mean of ensuring reliable and robust processes and conformity with good manufacturing practices. Apart from the commercialized hydrochloride dihydrate salt, the literature presents other five crystalline forms of minocycline with lower melting temperatures. Mendes *et al.* (7) report three crystalline polymorphic forms of this antibiotic by dissolution and/or suspension of amorphous minocycline base in organic solvents (ethers, esters or alcohols), followed by crystallization from the mixture. The three polymorphs were characterised by distinctive X-ray diffraction patterns and infrared spectra. Xiurong *et al.* (8) describe two other stable minocycline hydrochloride hydrate crystal forms obtained through consecutive steps of dissolution, crystallization, and drying of minocycline hydrochloride in a binary mixture of alcohol and water. Both polymorphs were differentiated by characteristic diffraction patterns and thermograms.

The selection of the most interesting polymorphs usually faces a dichotomy: on one hand the thermodynamically most stable form is preferred from a process control perspective; on the other hand, metastable polymorphs may have more interesting physical-chemical properties, such as melting point, bulk density, apparent solubility and dissolution rate, ultimately determining the drug stability, manipulation, and bioavailability (9,10). Therefore, the key-factor for a reliable manufacture in terms of the crystallization process lies in the careful evaluation of both thermodynamic and kinetic parameters, aiming the optimum therapeutic properties with best process control and storage stability.

Technologies involving supercritical CO_2 have been showing great potential regarding the control of the crystalline form of APIs (11). Furthermore, the miscibility of CO_2 with organic solvents provides alternative media for molecular recognition events, enabling consequently the assembly of novel crystalline structures, either polymorphs or cocrystals (12–15). Several polymorphs have been produced by recrystallization with supercritical CO_2 (14,16–20) some of each are unique, i.e. have not yet been produced by any other recrystallization technique (14,17,20). Most of these polymorphs were obtained using the well-known Supercritical Antisolvent (SAS) process. Briefly, the SAS process consists in dispersing a liquid solution (typically through a nozzle) into supercritical CO_2 (2,3,5,6,9,10). Crystallization is therefore the consequence of supersaturation driven by the dissolution of CO_2 in the liquid and subsequent extraction of the solvent into the supercritical phase (21). Conventional SAS processes require large volume high-pressure equipment to perform these mechanisms, which is a drawback. Yet an alternative has been proposed that enables the exploitation of the antisolvent properties of CO_2 in conventional spray-dryers by replacing the nozzle (ASAIS process (14)).

The antisolvent properties of CO_2 have been used before to precipitate minocycline. Cardoso *et al.* (22) have used the SAS process to micronize minocycline hydrochloride into amorphous particles. It is difficult to control the crystalline form using the SAS process because antisolvent crystallization and solvent extraction occur simultaneously in the precipitator, and therefore it is difficult to control competing supersaturating mechanisms, which may lead to crystalline or amorphous particles depending on subtle modifications in the process conditions (14,21,23).

In this work, minocycline hydrochloride was recrystallized in solution or suspension in three separated steps to enable better control over its crystallinity: addition of CO_2, recrystallization under stirred conditions, and solvent extraction. This process originated a new minocycline crystalline polymorph, which recrystallized in ethanol-CO_2 solutions as a dark-red precipitate. This novel crystalline form was extensively characterized, revealing a particularly high melting point of 247°C. To distinguish this polymorph that recrystallizes by the antisolvent effect of supercritical CO_2, we thereby designate it as β-minocycline hydrochloride (βMH) from this point forward.

EXPERIMENTAL METHODS

Materials

Minocycline chlorohydrate was kindly provided by AtralCipan (Portugal). Absolute ethanol (99.5%) was supplied

by Panreac (Spain) and was used as received. Carbon dioxide 99.98% pure was supplied by Air Liquide (Portugal).

Phase Equilibrium Studies

The precipitation of minocycline hydrochloride from ethanol solutions was carried out in the experimental setup schematically described in Fig. 1. The recrystallization visual cell (RVC) is represented in more detail in Fig. 2. It consists essentially of an 8 cm^3 stainless-steel high-pressure vessel with a borosilicate glass window (Maxos™, Auer Lighting, Germany), with an inlet and outlet ports. Pressure and temperature were measured using, respectively, a pressure transducer (Omega model PX603) and a T-type thermocouple assembly (Omega). The system pressure was controlled by a Newport Compressor (model 46-13421-2) and a back-pressure regulator (Tescom, model 26-1722-24). The RVC was kept in a temperature controlled air chamber by using a temperature controller Ero Electronic (model LDS) and a T-type thermocouple (Omega).

Three initial concentrations of minocycline hydrochloride in ethanol were studied: 5, 10 and 20 mg/g. One gram of each minocycline hydrochloride solution was loaded into the RVC. The cell was pressurized with CO_2 in small steps, corresponding to a pressure increase of approximately 0.2 MPa, each followed by a phase-equilibrium stabilization period of approximately 10 min with stirring (at 200 rpm) by means of a magnetic stirrer (Selecta, model Agimatic-N). The procedure was repeated until the formation of a precipitate was observed. Preliminary runs were performed to determine roughly the precipitation pressure. Afterwards, each point was repeated at least in triplicate and standard deviations were calculated. The phase equilibrium of ethanol and CO_2 was calculated using the Peng-Robinson equation of state (PR-EOS). The interaction parameter used in this calculation was obtained from experimental data published in a previous work (23). The calculations were made using the Matlab software (MathWorks, USA).

Minocycline Recrystallization in Suspension

Minocycline hydrochloride (αMH)/ethanol mixtures in mass proportion of 1:10 (100 mg of αMH to 1 g of ethanol) were loaded in the recrystallization visual cell schematically shown in Fig. 2. Because the minocycline composition in the mixture was much higher than the solubility limit in ethanol – we visually observed its precipitation when concentration reached approximately 5 mg/g by saturating 1.0 g of ethanol – a suspension was formed. This suspension was then mixed with CO_2 until the working pressure reached 8 MPa (at 50°C). The mixture was stirred at 200 rpm during the entire experiment. The recrystallization time was 2 h in all runs. Afterwards, 50 l of fresh CO_2 flowed through the RVC (with a flow-rate of 2 l/min) to remove the ethanol. Afterwards, the high-pressure vessel was slowly depressurized and the resulting material was collected from the vessel. Experiments were also carried out using N_2 instead of CO_2 under similar experimental conditions as a negative control of the antisolvent effect. The samples were stored in a closed desiccator prior to their characterization.

Differential Scanning Calorimetry (DSC)

Thermal analysis was performed using a Thermal Advantage differential scanning calorimeter Q1000 V9.8 (TA instruments-Waters, LLC) that was calibrated for temperature and cell constants using indium and sapphire. Samples (1–2 mg) were crimped in non-hermetic aluminium pans (30 μl) and scanned at a heating rate of 10°C/min in the range 25–200°C under a continuously purged dry nitrogen atmosphere (with flow rate of 50 ml/min). The instrument was equipped with a refrigerated cooling system. The data were collected in triplicate for each sample and were analysed using TA Instruments Universal Analysis 2000 V4.3A software.

Powder X-ray Diffraction (PXRD)

X-ray powder data were collected in a D8 Advance Bruker AXS θ–2θ diffractometer, with copper radiation (Cu Kα, λ= 1.5406 Å) and a secondary monochromator. The tube voltage and amperage was 40 kV and 40 mA, respectively. Each sample was scanned with 2θ between 5° and 35° with a step size of 0.01° and 0.5 s at each step.

Fourier Transform Infrared Spectroscopy (FTIR)

Dry samples of the new polymorph as well as the commercial minocycline were mixed with pure potassium bromide (KBr) powder and pressed. The FTIR spectra of the KBr pellets were obtained using a Mattson Satellite spectrometer, over the wave number range from 400 to 4,000 cm^{-1} at a resolution of 4 cm^{-1}, with an average accumulation of 100 scans.

Determination of the Chloride Content by Ion Exchange Chromatography

The chloride content in the minocycline hydrochloride samples was determined from a calibration curve by using an ion exchange chromatograph Dionex (USA) model DX-120 provided with an AS14A column and an Anion Self-Regenerating Suppressor ASRS300, eluted with a 1 ml/min flow of an 8 mM sodium carbonate and 1 mM sodium bicarbonate solution.

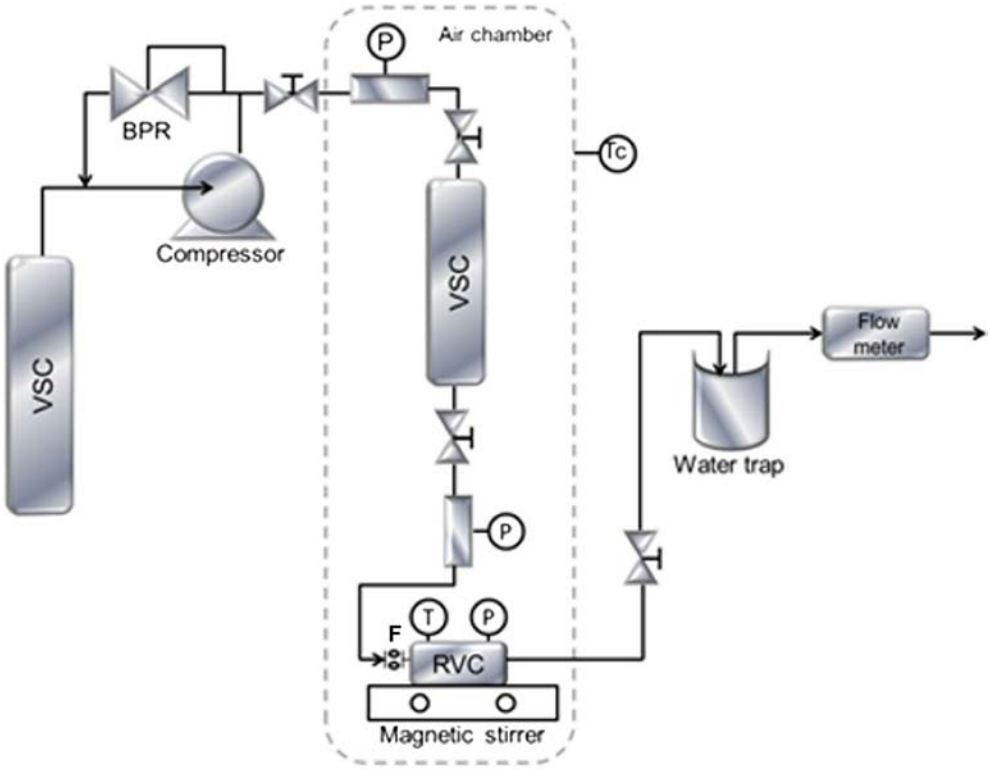

Fig. 1 Schematic diagram of experimental setup. VSC vessel storage cylinder; BPR back-pressure regulator; RVC recrystallization visual cell; F porous filter; T temperature indicator. P pressure indicator; Tc temperature controller.

Water Determination Using Karl Fischer Titration

The water content in the minocycline hydrochloride samples was measured by Karl Fischer titration using an 831 KF coulometer apparatus with a 728 magnetic stirrer (Metrohm). This technique was introduced by Karl Fischer in 1935 (24) and improved by other authors as described elsewhere (25).

Three different samples were analyzed: raw minocycline (αMH), and particles obtained by recrystallization using N_2 and using CO_2. Each sample was dissolved in dichloromethane in a concentration of 1 mg/ml and then 300 μl of this solution was injected into the Karl Fischer apparatus. A blank assay was performed by determining the water mass of dichloromethane. The analyses were performed in triplicate and the results averaged for the water mass in each sample.

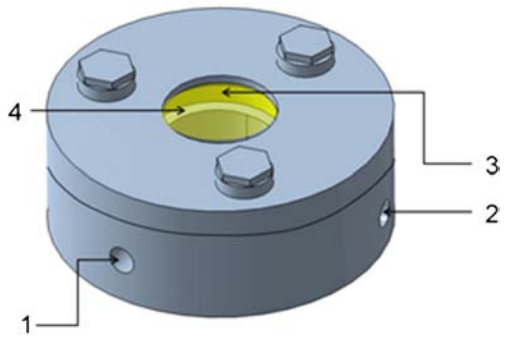

Fig. 2 Recrystallization visual cell. 1 inlet; 2 outlet; 3 glass window; 4 sealant O-ring.

^{15}N and ^{13}C Solid-State NMR

Powdered samples of the β-minocycline (~200 mg) were packed into 7 mm o.d. cylindrical zirconia rotors. ^{15}N cross polarization/magic angle spinning (CP/MAS) and ^{13}C CP/MAS spectra were obtained at 30.42 MHz and 75.49 MHz, respectively, on a Tecmag Redstone/Bruker 300 WB spectrometer, at a rate of 3.5 kHz with 90° RF pulses of about 6 μs and 4 μs, contact time of 3 ms and 1 ms, correspondingly, and a relaxation delay of 3 s. The significant contributions of the ^{13}C spinning side bands, particularly in the aromatic and carbonyl regions, were evaluated by comparing spectra run with and without the SELTICS sequence (Sideband Elimination by Temporary Interruption of Chemical Shift) (26). CP/MAS spectra with suppression of ^{13}C non-quaternary signals were achieved by interrupting proton decoupling during 40 μs before the acquisition period. Protonated ^{15}N signals were also suppressed in part using the same RF sequence and a 40 μs delay (total suppression were observed with a delay of 650 μs). ^{15}N and ^{13}C chemical shifts were referenced with respect to external glycine ($^{15}NH_2$ observed at 32.4 ppm in the liquid NH_3 scale, and ^{13}CO observed at 176.03 ppm). Typically, each spectrum was recorded in about two hours in order to accumulate 2,400 transients.

Relative Humidity Stability Analysis

Relative humidity (RH) conditions were achieved at ambient temperature (20°C) within sealed glass desiccator jars containing P_2O_5, for the 0% RH condition, and a saturated solution of $CuSO_4.5H_2O$, for 90%. Relative humidity conditions were monitored with humidity-indicator cards (Sigma-Aldrich). To compare the stability of α-minocycline hydrochloride to that of β-minocycline, open paper dishes containing 120 mg of powder were stored in the RH chambers at ambient temperature. A dish was removed for each material at each time point.

RESULTS

Recrystallization of Minocycline with CO_2

β-Minocycline precipitated in solution as a dark-red precipitate. After drying, it was recovered as a dark orange powder. The antimicrobial activity runs (not presented here) revealed that the recrystallized minocycline (β-minocycline) retained complete anti-microbial activity upon dissolution – the inhibition halos observed for raw minocycline hydrochloride were equivalent to those obtained with the new minocycline polymorph for all the reference antibiotic-susceptible isolates and the multidrug resistant isolates experimented.

Figure 3 shows equilibrium solubility of minocycline in mixtures of β-minocycline-ethanol-CO_2 measured experimentally and the corresponding CO_2 composition calculated from the Peng-Robinson equation of state. Figure 3 (a) shows that the precipitation pressure increases with increasing temperature, albeit the CO_2 liquid composition required to precipitate minocycline (at constant initial composition) was little sensitive to temperature in the range experimented here [see Fig. 3 (b)]. When the minocycline composition was 5 mg/g, the precipitation occurred in the vicinity of the critical point (where dV/dP tends to infinite) and therefore the composition could not be calculated using an equation of state.

β-Minocycline could also be recrystallized from suspensions of minocycline hydrochloride in CO_2-ethanol mixtures. However, we observed the reconversion of the dark red precipitate to the original yellow color during the depressurization of the system. Minocycline could only be recovered in the red crystalline form when the suspension was dried before depressurization by circulating 50 l of dry CO_2.

β-Minocycline Characterization

β-Minocycline was thoroughly characterized using several techniques. Figure 4 shows comparative PXRD diffractograms of the raw minocycline hydrochloride (αMH) and the new minocycline polymorph. Clearly distinctive peaks

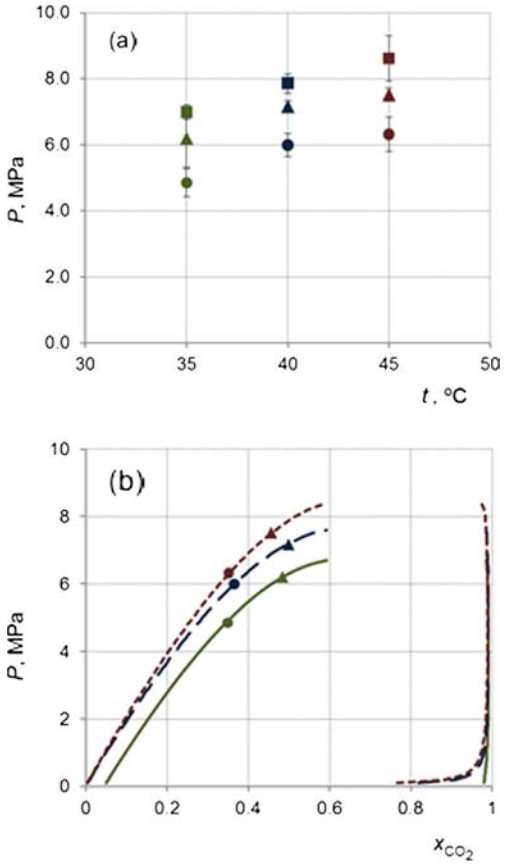

Fig. 3 Precipitation of minocycline hydrochloride from CO_2-ethanol mixtures for initial minocycline concentrations of 5 mg/g (*black square*), 10 mg/g (*black triangle*), and 20 mg/g (*black circle*). **(a)** pressure-temperature of observed precipitation points; **(b)** calculated liquid composition of CO_2 at precipitation conditions, using the Peng-Robinson equation of state. Lines correspond to calculated equilibrium CO_2-ethanol isotherms at 35°C (solid line), 40°C (long dashed line), and 45°C (short dashed line).

can be observed at 5.5, 9.6, 11.0, 13.5, 15.6, 15.8, 16.5, 16.8, 17.4, 18.3, 19.0, 19.2, 20.8, 22.0, 22.2 e 23.3±0.2° 2θ, being the most evident peak at 9.6 θ.

β-Minocycline is also characterized by having distinctive IR peaks at 1664, 1617, 1583, 1510, 1460, 1405, 1343, 1291, 1214, 1193, 1131, 1094, 1044, 1002, 973, 957, 876, 831, 717, 755, 670, 576 e 544±4 cm^{-1}, as Fig. 5 (b) shows. Small differences may be found in the IR spectra when comparing raw minocycline hydrochloride with β-minocycline. The absorption bands of the raw material are represented by sharp peaks and are assigned to the O-H and N-H stretching vibrations (3,480–3,355 cm^{-1}), whereas in β-minocycline these absorption bands (3,434–3,253 cm^{-1}) are broader. α-Minocycline hydrochloride range of peaks [see Fig. 5 (a)] are well separated from the O-H and N-H bands, probably due to the presence of Csp^2-H and Csp^3-H stretching vibrations (3,089–2,879 cm^{-1}), whilst the new polymorph shows a more extended set of corresponding peaks (2,998–2,780 cm^{-1}). Furthermore, an inversion in the intensity of the peaks concerning the conjugated C=O and C=C absorptions bands can be observed from α-

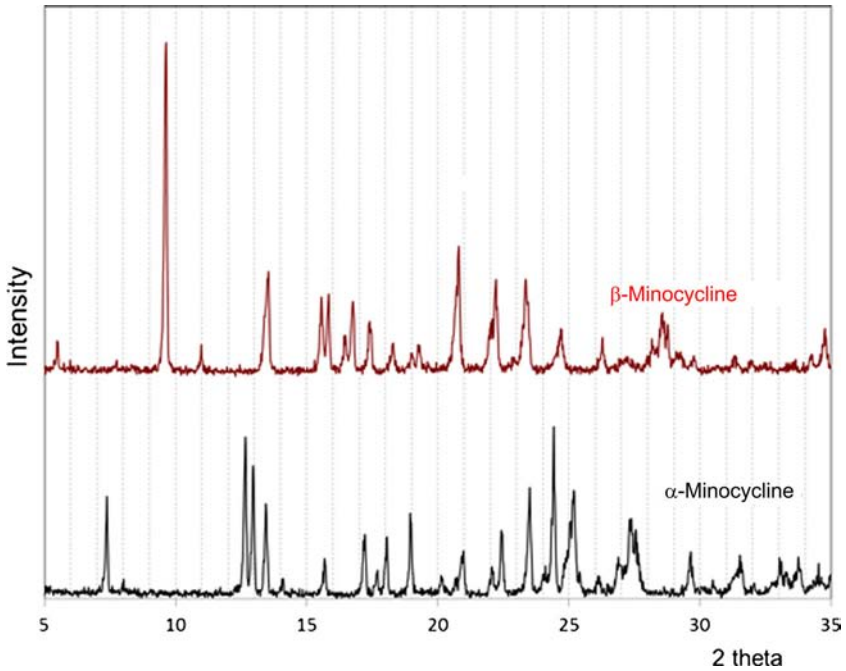

Fig. 4 PXRD diffractograms of minocycline hydrochloride (before recrystallization – commercial, unprocessed product) and of the new minocycline polymorph after 2 h recrystallization in a CO_2-ethanol suspension.

minocycline hydrochloride to β-minocycline. In the latter, the first peak (1,617 cm^{-1}) is weaker than the second peak (1,583 cm^{-1}), an opposite profile found for the former minocycline hydrochloride where the first peak (1,601 cm^{-1}) is stronger than the second one (1,586 cm^{-1}).

The chemical analyses revealed that all the recrystallized minocycline forms are chloride salts with 1:1 stoichiometry. However, the water content of β-minocycline is one third of the water content of the other forms, showing that minocycline lost most of its water during the recrystallization step with CO_2. The stoichiometry of the common (yellowish) minocycline hydrochloride corresponds approximately to 2 water molecules per molecule of minocycline, as expected, while the stoichiometry of the new minocycline polymorph is 0.7.

Figure 6 compares the thermograms of the raw minocycline hydrochloride and of the β-minocycline. The raw product shows two endothermic peaks at 187°C and 197°C, approximately followed by its degradation. On the contrary, β-minocycline shows a single melting peak at 247°C and a significantly higher thermo-stability. Figure 7 shows that β-minocycline reverts back to the yellowish hydrochloride after approximately 3 days storage in a 90% RH atmosphere.

NMR Analysis of β-Minocycline Structural Modifications

^{15}N and ^{13}C solid-state NMR were used to obtain detailed information about eventual structural modifications when comparing the raw minocycline hydrochloride with the new minocycline polymorph. Firstly, we must point out that tetracyclines comprise two different π-electronic systems (chromophores): a smaller one located on ring A, and a larger one located on rings BCD. Also, minocycline is the only tetracycline that has a $N(Me)_2$ group para to the aromatic phenol (see Scheme 1) and the π-electronic system of the BCD-chromophore is slightly perturbed by the electron donating $N(Me)_2$ group. It is generally accepted that the fully protonated species (Scheme 1) adopts a geometry different from that of the completely deprotonated species (27).

To our knowledge, the first ^{15}N CP/MAS study of tetracyclines was reported by Curtis and Wasylishen (28) who demonstrated that ^{15}N is a sensitive probe of the protonation of the A ring of tetracyclines. Figure 8 shows ^{15}N CP/MAS spectra recorded from raw minocycline hydrochloride and β-minocycline. The final chemical shifts are presented in Table I.

Only three ^{15}N resonances were observed on the CP/MAS of α-minocycline hydrochloride spectrum, which were assigned to the N,N-dimethylamino nitrogens attached at the C_7 position of the aromatic D ring (49.8 ppm), at the C_4 position of the A ring (41.9 ppm), and to the amide group $CO^{15}NH_2$ (99.8 ppm). These results agree well with previous reported data on minocycline hydrochloride (see Table I) (29). Figure 8 also shows ^{15}N CP/MAS spectra from β-minocycline (b) and α-minocycline hydrochloride (d) which were run with 40 μs dipolar dephasing before the acquisition period. The selection of a dipolar dephasing delay short enough to enable recording NH_2 signals facilitates observing the trend followed by other resonances when submitted to that delay. Accordingly, it is observed an intensity decrease of the three ^{15}N minocycline hydrochloride signals while for β-minocycline the resonance at lower frequency (24.4 ppm) is

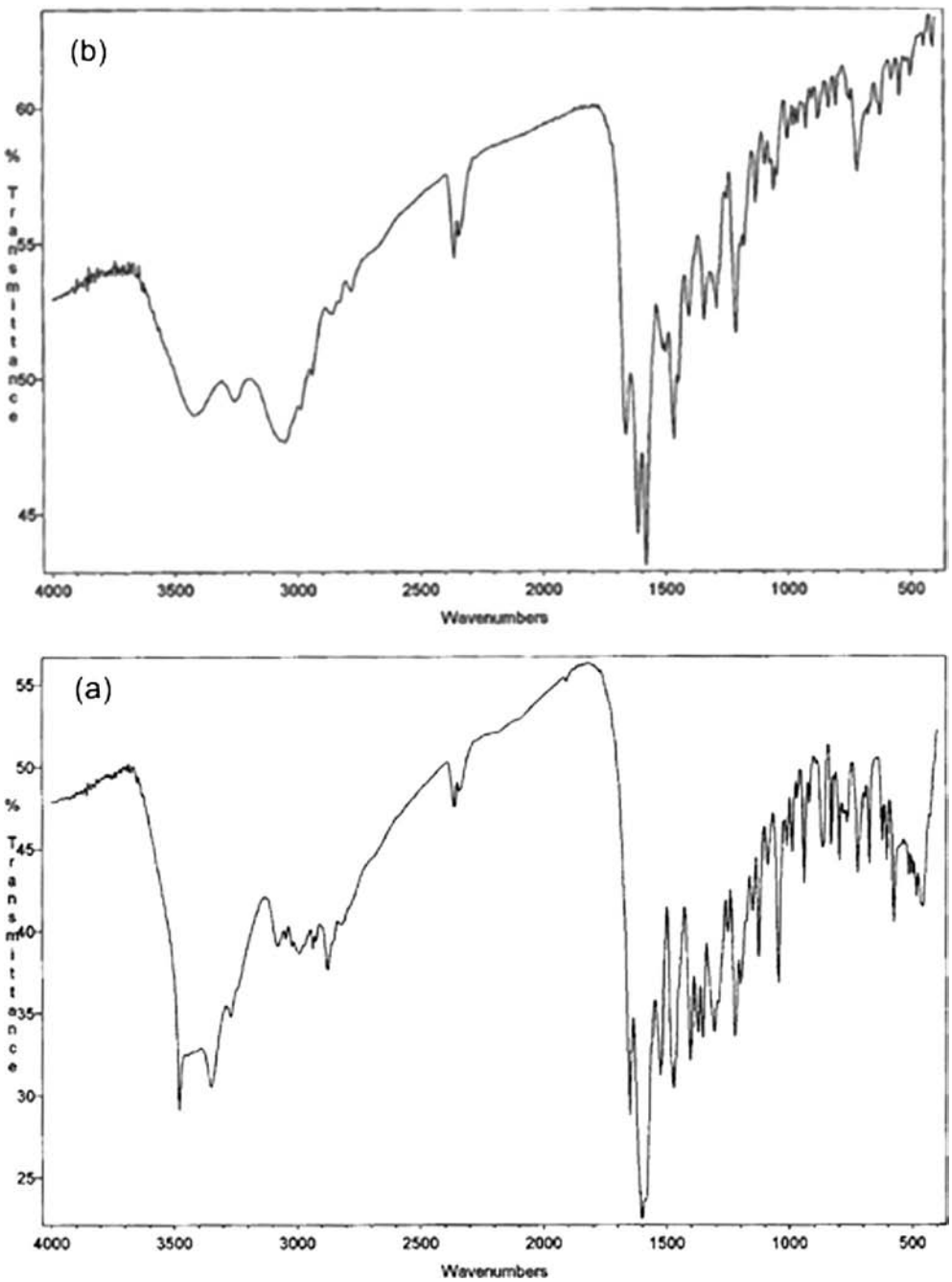

Fig. 5 FTIR spectra: **(a)** α-minocycline hydrochloride; **(b)** β-minocycline hydrochloride.

not affected. This result clearly shows that in β-minocycline one N $(\underline{C}H_3)_2$ only is protonated that, at this stage, is not possible to assign unequivocally. Also, ^{15}N signal at 48.4 ppm may be assigned to deprotonated 4-N$(\underline{C}H_3)_2$ or 7-N$(\underline{C}H_3)_2$. Moreover, the fact that the signal of the NH_2 group of β-minocycline is observed at a frequency (120.7 ppm) higher than the signal of the NH_2 group of raw minocycline (99.8 ppm) is consistent with a modification of the involvement of NH_2 in hydrogen bonding when compared with raw minocycline. ^{15}N chemical shift is more sensitive to the presence of the hydrogen bonds than ^{13}C due to the wider chemical shift range of the former. For the ^{15}N isotropic chemical shift, the protonation induced shifts are of the order of about 25 ppm toward higher frequencies for aliphatic amines (30).

Further elucidation on the structures of both minocyclines was obtained from ^{13}C CP/MAS spectra. Figure 9 shows relevant ^{13}C CP/MAS spectra of α-minocycline hydrochloride and of the new polymorph obtained with elimination of spinning side bands. Two spectra are presented for each minocycline thus enabling to identify signals from strongly dipolar coupled nuclei (CH and CH_2). These signals are suppressed in Fig. 9 (b) (the spectra were acquired using a

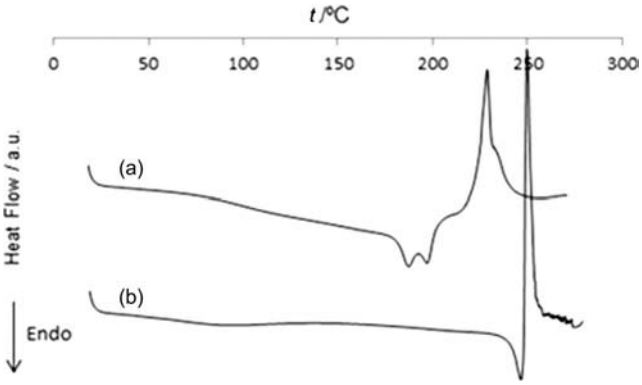

Fig. 6 DSC thermograms: **(a)** raw minocycline hydrochloride; **(b)** β-minocycline hydrochloride.

RF sequence that enables observing only quaternary and methyl resonances), whilst Fig. 9 (a) shows all the resonances. The corresponding chemical shifts are listed in Table I. The assignments of the α-minocycline and of the β-minocycline spectra were primarily based upon comparison to solution (31–35) and solid-state results (29). Previous assignments from solid studies are also shown in Table I. ^{13}C CP/MAS technique was already used to obtain high resolution solid-state ^{13}C NMR spectra of several tetracycline antibiotics (29).

Both ^{13}C CP/MAS spectra are assigned to crystalline compounds, in the NMR scale, with one molecule in the unit cell because only one resonance is assigned to each carbon species. All signals are well resolved, except those from carbons bound to ^{14}N (e.g. C_4, 2-$\underline{C}ONH_2$), because of the extent of dipolar broadening due to the neighboring quadrupolar nuclei. The chemical shifts of the minocycline hydrochloride (αMH) are very similar to previous data reported by Curtis and Wasylishen (28), as pointed out for ^{15}N data (Table I). Therefore, at this stage, αMH is considered to be a fully protonated form of minocycline with two possible tautomeric forms of the amide substituent. Subsequently, by comparison with the chemical shifts obtained for doxycycline hydrochloride (28) which crystallizes with two molecules per unit cell, each one with a different tautomeric form, we may conclude that the chemical shift of C_2 (99.82 ppm, see Table I) is consistent with the presence of the tautomeric form 1 of Scheme 2. ^{13}C CP/MAS spectrum of αMH agrees well with the presence of a single molecule with four inequivalent amino-methyl groups, not to the presence of two different tautomeric forms, because only one resonance was obtained for each one of all the other carbon species. Thus, are assigned two signals to methyl groups in 7-N$(CH_3)_2$ and two signals to methyl groups in 4-N$(CH_3)_2$. However, it must be pointed out here that elsewhere (28) only two chemical shifts were indicated for the amino-methyl groups, presumably for 4-N$(CH_3)_2$, the group that is present in all tetracyclines.

In a first approach, these are the most important differences between minocycline hydrochloride (αMH) and β-minocycline (βMH) spectra:

a) Low field (high frequency) shifts are observed for all the resonances of β-minocycline except in the positions of C_2, C_9, C_{12} and C_{12a}, not taken the methyl groups into account.
b) In the region 20–60 ppm: αMH presents six well-resolved resonances and βMH four only.
c) In the region 120–150 ppm: αMH shows signals at 120.20 ppm and 133.47 ppm, while βMH presents resonances at 143.2 ppm and 140.3 ppm.
d) In the region 170–200 ppm: the asymmetric signals from 2-$\underline{C}ONH_2$ are observed at 171.32 ppm and 174.57 ppm for αMH and βMH, respectively, and the signals from C_1, C_3 and C_{11} are all shifted to higher frequencies in βMH when compared with those in αMH.

These observations are consistent with changes in βMH, namely:

a) Methyl resonances from 4-N$(CH_3)_2$ equivalent to 7-N$(CH_3)_2$ signals.
b) Electronic changes induced in ring D.
c) Hydrogen bond rearrangements.

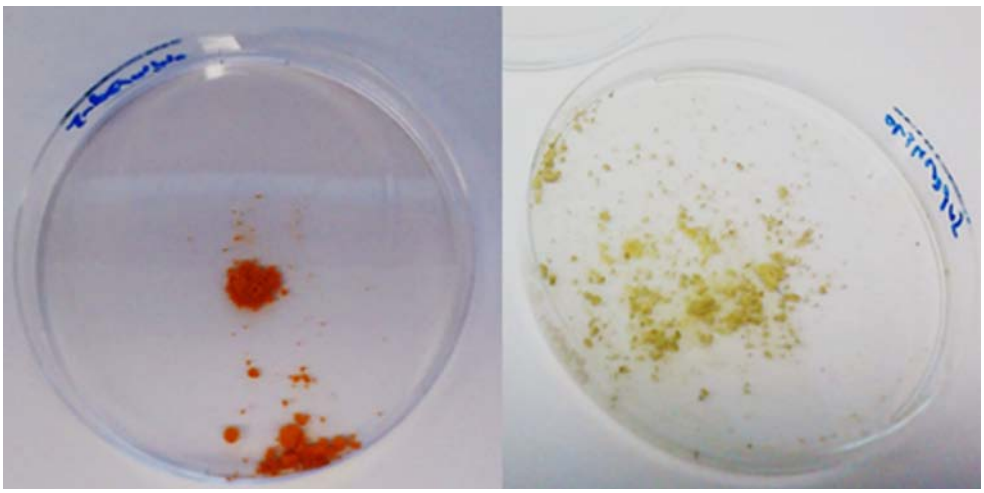

Fig. 7 Relative Humidity (RH) stability of β-minocycline hydrochloride. Appearance before (left) and after (right) 72 h in 90% RH.

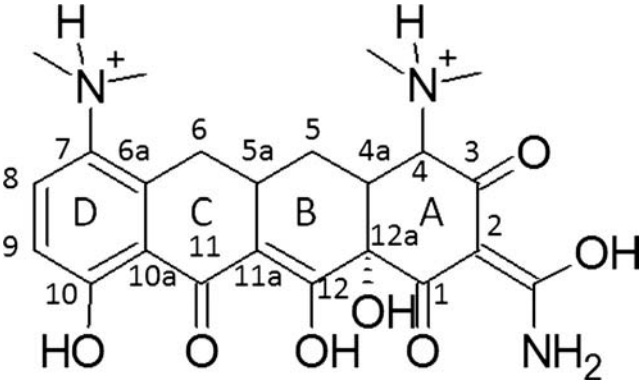

Scheme 1 Chemical structure of fully protonated α-minocycline hydrochloride.

Therefore, in β-minocycline, ^{13}C CP/MAS NMR shows that deprotonation of the C_7-$N(CH_3)_2$ group is particularly noticeable by the observed changes in the D ring resonances: strong deshielding of C_{6a} and C_7 (−6.80 and−9.72 ppm, respectively) and shielding of C_9 (3.87 ppm, which is due to the γ-shielding effect). On the other hand, the C_1 high frequency shift (−6.48 ppm) points to hydrogen bonding involving C_1O and 2-$COHNH_2$ (174.57 ppm), as shown in form 2 of Scheme 2, not NH_2 in the amide group (form 1 of Scheme 2). Also, the chemical shifts observed for C_{11} and C_{12} (194.96 and 171.98 ppm) are consistent with no hydrogen bonding between $C_{11}O$ and HOC_{12}. In the αMH spectra, C_{11} and C_{12} are observed at 193.96 and 176.93 ppm, respectively, which is an indication that HOC_{12} may be involved in hydrogen bonding to $C_{11}O$. The C_4 signal has similar shape in both minocycline spectra and the corresponding chemical shift differs only by 0.98 ppm. Thus, the effect of ^{14}N on the C_4 resonance is analogous in both compounds and this feature is consistent with the 4-$N(CH_3)_2$ groups being protonated in both minocyclines.

Taking into account the conclusions obtained from ^{15}N and ^{13}C CP/MAS NMR data, it is proposed here that the chemical structure for β-minocycline is that shown in Scheme 3. Moreover, the conformations of the amide substituent in the ring A of the raw minocycline and of the β-

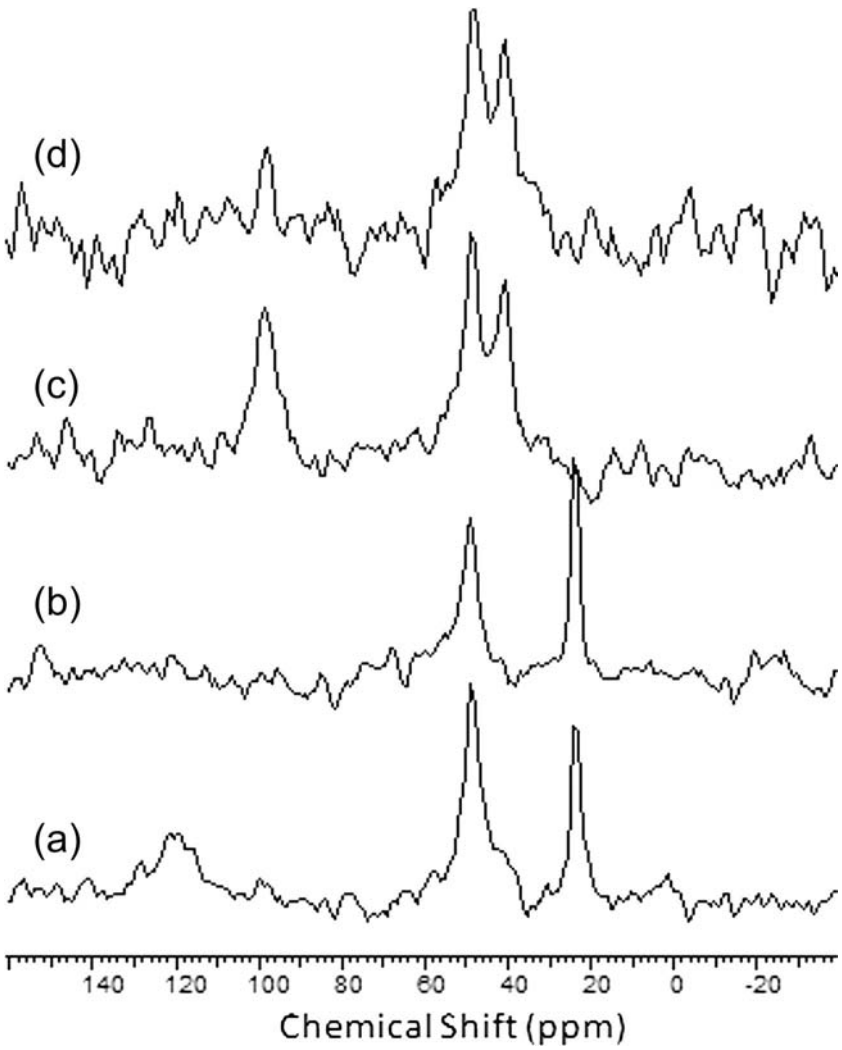

Fig. 8 ^{15}N CP/MAS spectra obtained from β-minocycline hydrochloride **(a, b)** and from α-minocycline hydrochloride **(c, d)** without **(a, c)** and with 40 μs dipolar dephasing before the acquisition period **(b, d)**.

Table I ^{15}N CP/MAS and ^{13}C CP/MAS chemical shifts of α-minocycline hydrochloride (δ_1) and of β-minocycline hydrochloride (δ_2) obtained in this study and reported on the indicated references for α-minocycline hydrochloride. The chemical shift differences ($\delta_1 - \delta_2$) are also shown in underlined and bold formats for rings B and D, respectively, while the corresponding data for rings A and C are depicted in the usual format

	^{13}C (δ)/ppm *^{15}N (δ)/ppm* (this study)			^{13}C (δ)/ppm *^{15}N (δ)/ppm* (from refs.28,29)
Carbon number	δ_1	δ_2	$\delta_1 - \delta_2$	
1	189.12	195.60	−6.48	189.5
2	99.82	98.86	0.96	100.2
2-CONH$_2$	171.32 *99.0*	174.57* *120.7*	−3.25 *−21.7*	171.2 *99.8* (29)
3	186.53	187.84	−1.31	187.0
4	68.11	69.09	−0.98	68.9
4a	35.10	38.03	−2.93	35.6
4-*N*(CH$_3$)$_2$	38.99/43.19 *41.2*	44.50/47.73 *48.4*	−5.51/−4.54 *−7.2*	39.5/43.8 *41.9* (29)
5	~28	~30	−2	27.4
5a	31.22	33.17	−1.95	31.9
6	35.10	38.03	−2.93	35.6
6a	133.47	140.27	**−6.80**	133.9
7	133.47	143.19	**−9.72**	133.9
7-*N*(CH$_3$)$_2$	46.43/49.99 *49.2*	44.50/47.73 *24.4*	**1.93/2.26** ***24.8***	– *49.8* (29)
8	129.91	130.24	**−0.33**	130.4
9	120.20	116.33	**3.87**	120.7
10	158.38	159.04	**−0.66**	158.8
10a	114.70	116.33	**−1.63**	115.3
11	193.97	194.96	−0.99	194.4
11a	108.23	109.53	−1.3	108.7
12	176.83	171.98	4.85	177.2
12a	75.87	75.24	0,63	76.4

* This assignment was based on the observed signal broadening due to the interaction with ^{14}N, a quadrupolar nucleus

minocycline appear to be similar to forms 1 and 2 of Scheme 2, respectively.

It is worth mentioning that additional structural elucidation on minocyclines could be obtained from solid-state NMR experiments using more sophisticated techniques that generally require higher magnetic fields and fast MAS. Examples of these techniques are novel ^{15}N-edited and 2D ^{14}N-^{1}H solid-state NMR (36), to probe intermolecular interactions and nitrogen protonation, or ^{14}N-^{1}H HMQC solid-state NMR (37) or high-resolution ^{1}H double-quantum solid-state NMR spectroscopy (38), to probe hydrogen bonding.

Future work will be performed in order to solve the β-minocycline structure using either PXRD or PXRD in combination with solid-state NMR data. In the latter case, crystal structure determination from PXRD data will allow the calculation of the NMR data using density functional theory-based techniques, with the structure validated by seeking agreement with experimental NMR data, as shown in recent studies (39,40).

DISCUSSION

The results presented here evidence that carbon dioxide acted as an antisolvent, recrystallizing minocycline as a new hydrochloride crystal. The raw minocycline and the minocycline processed with N_2 show the same stoichiometry. Even though a significant current of anhydrous nitrogen circulated in the recrystallization cell, the water content was not reduced because the two water molecules should be in the crystalline lattice of the minocycline hydrochloride crystals. The new minocycline polymorph shows a much reduced water content, which also explains the clearly distinct PXRD and IR peaks (Figs. 4 and 5) (41). We were not able to produce the β-minocycline polymorph when CO_2 was replaced by N_2.

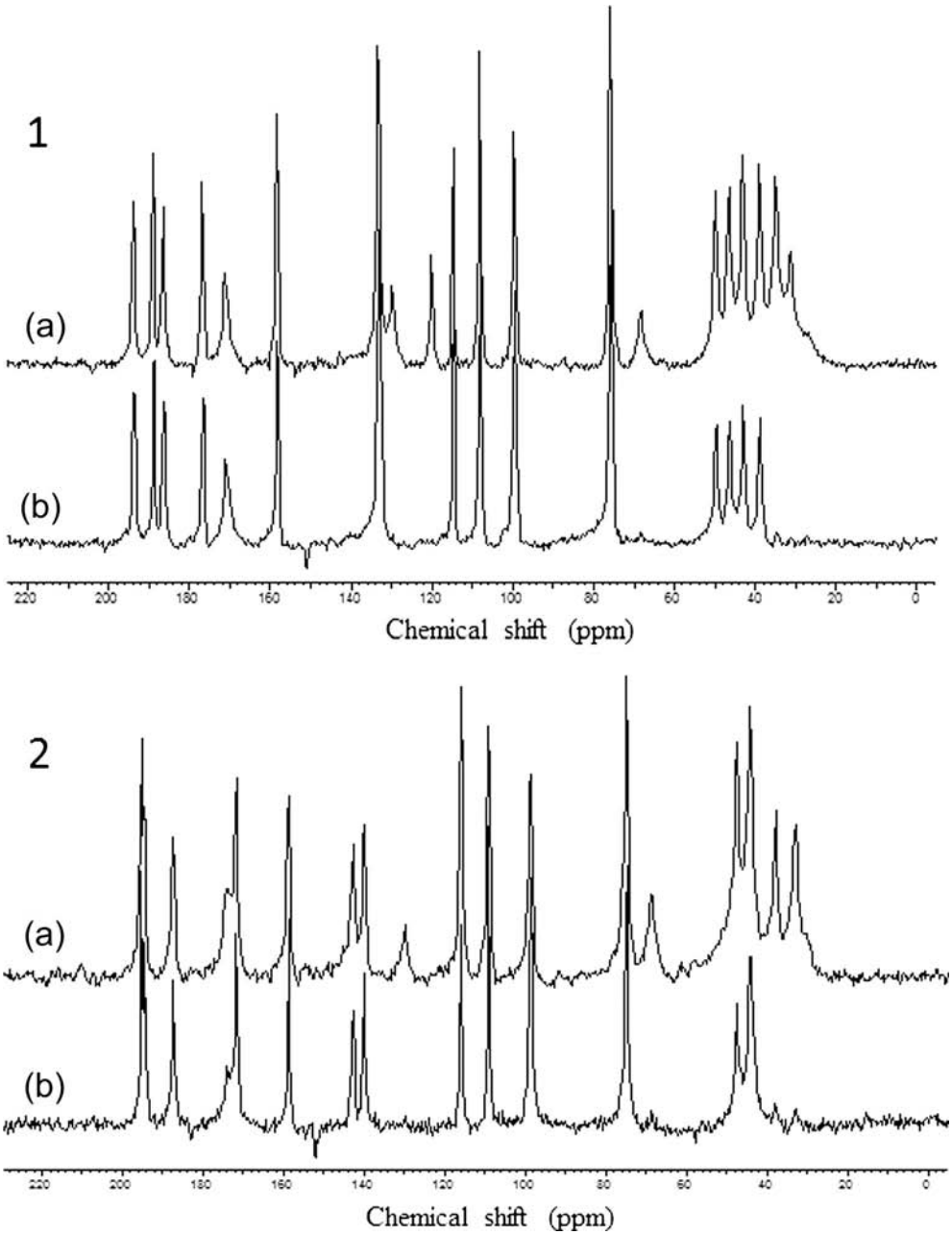

Fig. 9 ^{13}C CP/MAS spectra of α-minocycline hydrochloride (**1**) and of β-minocycline hydrochloride (**2**), which were recorded with elimination of spinning side bands: **(a)** showing all the carbon resonances; **(b)** not presenting CH and CH_2 signals (run with a non-quaternary carbon signal suppression pulse sequence).

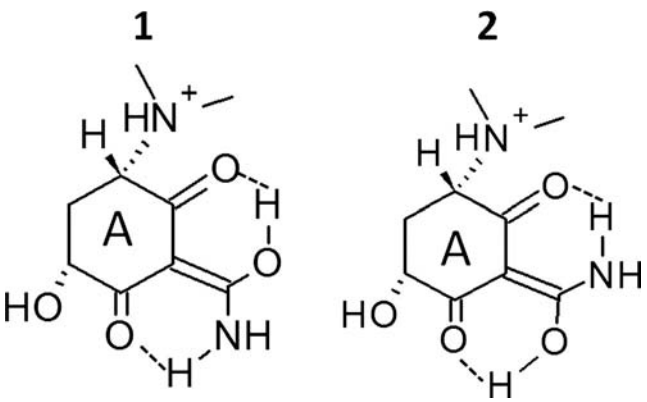

Scheme 2 Chemical structure of tautomeric forms of the amide substituent in ring A found in tetracycline hydrochloride salts (28).

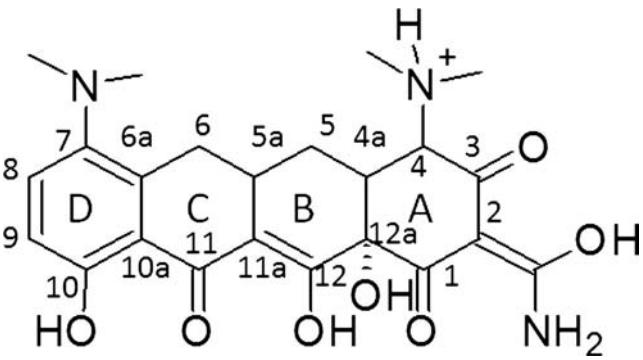

Scheme 3 Chemical structure of β-minocycline proposed in this study.

Table II Comparative analysis of the chemical composition of the raw minocycline hydrochloride (α-minocycline), β-minocycline hydrochloride and α-minocycline hydrochloride processed with N_2

	Composition (weight fraction)		Stoichiometry per molecule of minocycline ($C_{23}H_{27}N_3O_7$)	
	Water	Chloride	Water	Chloride
α-Minocycline hydrochloride	0.09	0.067	2.2	1.0
β-Minocycline hydrochloride	0.03	0.07	0.7	1.0
α-Minocycline hydrochloride recrystallized with N_2	0.10	0.067	2.5	1.0

This result emphasizes the importance of CO_2 antisolvent action on minocycline crystallization, as N_2 provides a negative control for this particular precipitation mechanism (14).

Others have already addressed the precipitation of minocycline hydrochloride by using a CO_2 antisolvent process (SAS) (22). Nevertheless it has been reported the preparation of amorphous hydrochloride precipitates only. This discrepancy of results emphasizes the importance of controlling thermodynamic and kinetic constraints, whenever a particular crystalline form is desired as herein, rather than simply aiming the micronization of the material as pursued by Cardoso *et al.* (22). The conditions required for precipitation of β-minocycline are shown in Fig. 3, wherein it is observed that the new minocycline polymorph precipitates in solution when an antisolvent composition is achieved. The antisolvent precipitation is progressive, i.e. low composition in minocycline requires higher composition of CO_2 in the liquid phase. Minocycline was therefore precipitating as it became increasingly diluted, because its solubility decreases as the volume of liquid increases due to the condensation of CO_2. Conversely, in the SAS process, the solvent is rapidly extracted and therefore supersaturation may be a consequence of increasingly concentrating solutions, similarly to a conventional spray-drying (14). This disfavors the formation of anhydrous minocycline because the water dissolved (approximately 9% as Table II shows), which was initially present in the hydrochloride structure, should also concentrate in solution, because the solvent (ethanol) is preferentially extracted, as it is far more soluble in supercritical CO_2.

β-Minocycline revealed substantial propensity to revert back to the hydrate form in a 90% RH atmosphere (Fig. 7). We also observed that the β-minocycline crystal was only obtained when the mixture was cleared from the ethanol and the crystallization water, by circulating a CO_2 stream (50 l) prior to the system depressurization. Since the aim of this work focused mostly on the characterization of the new polymorph, no systematic process optimization was carried regarding the crystallization kinetics and overall efficiency. Still, Fig. 4 shows that minocycline hydrochloride could also be recrystallized in suspension in relatively short time. After 2 h of recrystallization in suspension the raw hydrochloride dihydrate characteristic peaks could not be detected in the diffractograms of the samples; which could therefore be characterized as "PXRD pure" (see Fig. 4).

β-Minocycline was less stable at 90% RH than the initial hydrate, obviously because the last was already hydrated. Nonetheless, an overall higher chemical stability may be inferred from the much higher melting point of β-minocycline (247 °C compared to 197 °C or 187 °C) (see Fig. 6). The higher stability is particularly evident in the thermogram of Fig. 6 wherein the hydrochloride shows two clear peaks, suggesting that the sample is a mixture of crystalline polymorphs of minocycline hydrates. Solid-state NMR presented evidence for strong structural differences between α-minocycline and β-minocycline. The most important one is the presence of just one N-dimethylamino protonated nitrogen in β-minocycline while both nitrogens are protonated in minocycline hydrochloride. Considering that all the recrystallized minocycline forms are chloride salts with 1:1 stoichiometry and that both N-dimethylamino nitrogens are protonated in minocycline hydrochloride it is hypothesized here that, under acidic conditions, water was involved in the protonation of one of the nitrogens in the minocycline hydrochloride. Subsequent to water removal, this nitrogen was deprotonated giving β-minocycline which contains just one third of the water content.

The thermogram (Fig. 6) shows that β-minocyline is stable until its melting temperature is reached, degrading immediately afterwards. Notwithstanding, the 247 °C places minocycline in the top of the most heat-resistant antibiotics. The thermostability across a wider range of temperature may enable the development of new minocycline formulations by using processes involving high temperature, such as development of antibiotic composite materials by hot-melt extrusion or exothermic polymerization reactions.

Overall, we must also emphasize the potential of the ethanol-CO_2 system towards the production of anhydrous substances. The ability of supercritical CO_2 to extract water from hydroalcoholic mixtures has been previously reported (23,41). However, herein water molecules were extracted from the crystalline structure of an API by simply suspending it in ethanol-CO_2 mixtures under moderate pressure and temperature (8 MPa and 45 °C) for a relatively short period of time (2 h). Such conditions are easily attained by using conventional equipment that is typically employed in

extraction using supercritical CO_2. We therefore anticipate that this may be an alternative process to control the crystallinity of APIs and perhaps the intellectual property of more advanced pharmaceutical products.

CONCLUSIONS

A novel minocycline hydrochloride polymorph was discovered that shows a considerably higher thermostability (with a melting point of 247 °C) and crystalline homogeneity than the commercially available hydrochloride dihydrate salts. The recrystallization process results from the antisolvent properties of carbon dioxide and from the considerable affinity of water to ethanol-CO_2 mixtures. The results discussed here may drive two major lines of work: one regarding the formulation and applications of β-minocycline hydrochloride, and other regarding the use of the ethanol-CO_2 system as a route for producing anhydrous APIs.

ACKNOWLEDGMENTS AND DISCLOSURES

We thank Dr. William Heggie and Dr. Zita Mendes from Hovione FarmaCiencia SA (Loures, Portugal) for the fruitful discussions and Professor Aida Duarte for the invaluable help at Microbiology Laboratory of FFUL (Lisbon, Portugal). For financial support, the authors are grateful to Fundação para a Ciência e Tecnologia (FCT), Lisbon (Grants SFRH/BD/39836/2007 and PTDC/EQUFTT/099912/2008, Strategic Project PEst-OE/SAU/UI4013/2011, project RECI/QEQ-QIN/0189/2012) and "Infra-estruturas de C&T" for the funding of the upgrade of the solid-state NMR spectrometer.

REFERENCES

1. Bishburg E, Bishburg K. Minocycline – an old drug for a new century: emphasis on methicillin-resistant *Staphylococcus aureus* (MRSA) and *Acinetobacter baumannii*. Int J Antimicrob Agents. 2009;34:395–401.
2. Huang V, Cheung CM, Kaatz GW, Rybak MJ. Evaluation of dalbavancin, tigecycline, minocycline, tetracycline, teicoplanin, and vancomycin against community-associated and multidrug-resistant hospital-associated methicillin-resistant *Staphylococcus aureus*. Int J Antimicrob Agents. 2010;35:25–9.
3. Torrey EF, Davis JM. Adjunct treatments for schizophrenia and bipolar disorder: what to try when you are out of ideas. Clin Schizophr Relat Psychoses. 2012;5:208–16.
4. European Pharmacopoeia. 8th Ed. Strasbourg, France: Council of Europe; 2013. p. 2779.
5. Ahlneck C, Zografi G. The molecular basis of moisture effects on the physical and chemical stability of drugs in the solid state. Int J Pharm. 1990;62:87–95.
6. Waterman KC, Adami RC. Accelerated aging: prediction of chemical stability of pharmaceuticals. Int J Pharm. 2005;293:101–25.
7. Mendes Z, Antunes JR, Marto S, Heggie W. Crystalline minocycline base and processes for its preparation. WO2008102161-A2; US20100286417-A1.
8. Xiurong H, Jianming G, Linschen C. Minocycline hydrochloride hydrate crystal forms and preparation method thereof. CN101693669-A.
9. Morissette SL, Almarsson O, Peterson ML, Remenar JF, Read MJ, Lemmo AV, *et al.* High-throughput crystallization: polymorphs, salts, co-crystals and solvates of pharmaceutical solids. Adv Drug Deliv Rev. 2004;56:275–300.
10. Schultheiss N, Newman A. Pharmaceutical cocrystals and their physicochemical properties. Cryst Growth Des. 2009;9:2950–67.
11. Childs SL, Stahly GP, Park A. The salt-cocrystal continuum: the influence of crystal structure on ionization state. Mol Pharmaceutics. 2007;4:323–38.
12. Padrela L, Rodrigues MA, Velaga SP, Fernandes AC, Matos HA, Azevedo EG. Screening for pharmaceutical cocrystals using the supercritical fluid enhanced atomization process. J Supercrit Fluids. 2010;53:156–64.
13. Padrela L, Rodrigues MA, Velaga SP, Matos HA, Azevedo EG. Formation of indomethacin-saccharin cocrystals using supercritical fluid technology. Eur J Pharm Sci. 2009;38:9–17.
14. Rodrigues MA, Li J, Padrela L, Almeida AJ, Matos HA, Azevedo EG. Antisolvent effect in the production of lysozyme nano- and microparticles by supercritical fluid-assisted atomization processes. J Supercrit Fluids. 2009;48:253–60.
15. Tiago JM, Padrela L, Rodrigues MA, Matos HA, Almeida AJ, Azevedo EG. Single-step co-crystallization and lipid dispersion by supercritical enhanced atomization. Cryst Growth Des. 2013;13:4940–74.
16. Bettini R, Bonassi L, Castoro V, Rossi A, Zema L, Gazzaniga A, *et al.* Solubility and conversion of carbamazepine polymorphs in supercritical carbon dioxide. Eur J Pharm Sci. 2001;13:281–6.
17. Bettini R, Menabeni R, Tozzi R, Pranzo MB, Pasquali I, Chierotti MR, *et al.* Didanosine polymorphism in a supercritical antisolvent process. J Pharm Sci. 2010;99:1855–70.
18. Cocero MJ, Martin A, Mattea F, Varona S. Encapsulation and co-precipitation processes with supercritical fluids: fundamentals and applications. J Supercrit Fluids. 2009;47:546–55.
19. Martin A, Scholle K, Mattea F, Meterc D, Cocero MJ. Production of polymorphs of ibuprofen sodium by supercritical antisolvent (SAS) precipitation. Cryst Growth Des. 2009;9:2504–11.
20. Subra P, Laudani CG, Vega-Gonzalez A, Reverchon E. Precipitation and phase behavior of theophylline in solvent-supercritical CO2 mixtures. J Supercrit Fluids. 2005;35:95–105.
21. Reverchon E, Torino E, Dowy S, Braeuer A, Leipertz A. Interactions of phase equilibria, jet fluid dynamics and mass transfer during supercritical antisolvent micronization. Chem Eng J. 2010;156:446–58.
22. Cardoso MAT, Cabral JMS, Palavra AMF, Geraldes V. Characterization of minocycline powder micronized by a supercritical antisolvent (SAS) process. J Supercrit Fluids. 2008;47:247–58.
23. Li J, Rodrigues MA, Matos HA, Azevedo EG. VLE of carbon dioxide/ethanol/water: applications to volume expansion evaluation and water removal efficiency. Ind Eng Chem Res. 2005;44:6751–9.
24. Fischer K. A new method for the analytical determination of the water content of liquids and solids. Angew Chem. 1935;48:394–6.
25. Bruttel P, Schlink R. Water determination by Karl Fisher titration. Metrohm Ltd: Herisau, Switzerland; 2006.
26. Hong J, Harbison GS. Magic-Angle-spinning Side-band elimination by temporary interruption of the chemical-shift. J Magn Reson Ser A. 1993;105:128–36.
27. Stezwoski JJ. Chemical-structural properties of tetracycline derivatives. 1. Molecular structure and conformation of the free base derivatives. J Am Chem Soc. 1976;98:6012–8.

28. Curtis RD, Wasylishen RE. A nitrogen-15 nuclear magnetic resonance study of the tetracycline antibiotics. Can J Chem. 1991;69: 834–8.
29. Mooibroek S, Wasylishen RE. A carbon-13 nuclear magnetic resonance study of solid tetracyclines. Can J Chem. 1987;65: 357–62.
30. Levy GC, Lichter RL. Nitrogen-15 nuclear magnetic resonance spectroscopy. New York: John Wiley & Sons; 1979.
31. Casy AF, Yasin A. Application of ^{13}C nuclear magnetic resonance spectroscopy to the analysis and structural investigation of tetracycline antibiotics and their common impurities. J Pharm Biomed Anal. 1984;2:19–36.
32. Casy AF, Yasin A. Stereochemical studies of tetracycline antibiotics and their common impurities by 400 MHz ^{1}H NMR spectroscopy. Magn Reson Chem. 1985;23:767–70.
33. Mannargudi B, McNally D, Reynolds W, Uetrecht J. Bioactivation of minocycline to reactive intermediates by myeloperoxidase, horseradish peroxidase, and hepatic microsomes: implications for minocycline-induced lupus and hepatitis. Drug Metab Dispos. 2009;37:1806–18.
34. Mazzola EP, Melin JA, Wayland LG. ^{13}C-NMR spectroscopy of three tetracycline antibiotics: minocycline hydrochloride, meclocycline, and rolitetracycline. J Pharm Sci. 1980;69:229–30.
35. Takeuchi Y, Imafuku Y, Nishikawa M. Reassignment of the ^{13}C NMR spectrum of minomycin. Arkivoc. 2003; XV:2003:39–46.
36. Tatton AS, Pham TN, Vogt FG, Iuga D, Edwards AJ, Brown SP. Probing intermolecular interactions and nitrogen protonation in pharmaceuticals by novel ^{15}N-edited and 2D ^{14}N-^{1}H solid-state NMR. Cryst Eng Comm. 2012;14:2654–9.
37. Tatton AS, Pham TN, Vogt FG, Iuga D, Edwards AJ, Brown SP. Probing hydrogen bonding in cocrystals and amorphous dispersions using ^{14}N-^{1}H HMQC solid-state NMR. Mol Pharm. 2013;10:999–1007.
38. Bradley JP, Pickard CJ, Burley JC, Martin DR, Hughes LP, Cosgrove SD, *et al.* Probing intermolecular hydrogen bonding in sibenadet hydrochloride polymorphs by high-resolution ^{1}H double-quantum solid-state NMR spectroscopy. J Pharm Sci. 2012;101:1821–30.
39. Baias M, Widdifield CM, Dumez J-N, Thompson HPG, Cooper TG, Salager E, *et al.* Powder crystallography of pharmaceutical materials by combined crystal structure prediction and solid-state ^{1}H NMR spectroscopy. Phys Chem Chem Phys. 2013;15:8069–80.
40. Dudenko DV, Williams PA, Hughes CE, Antzutkin ON, Velaga SP, Brown SP, *et al.* Exploiting the synergy of powder X-ray diffraction and solid-state NMR spectroscopy in structure determination of organic molecular of solids. J Phys Chem C. 2013;117:12258–65.
41. Rodrigues MA, Padrela L, Matos HA, Azevedo EG, Pinheiro L, Bettencourt A, Castro ML, Almeida AJ, Duarte MA. New crystalline minocycline chlorohydrate, useful for preparing composite materials, prostheses, bone cements, implants, and controlled drug delivery formulations for the treatment of bacterial infections. WO2013095169-A1; PT106063-A1; 2013.